Received: 7 February 2020 | Revised: 16 August 2021 | Accepted: 27 October 2021

DOI: 10.1111/jfr3.12775

ORIGINAL ARTICLE

CIWEM Chartered Institution of Water and Environmental Management | Journal of Flood Risk Management | WILEY

Groundwater rebound and flooding in the Naples' periurban area (Italy)

Vincenzo Allocca | **Silvio Coda** | **Domenico Calcaterra** | **Pantaleone De Vita**

Department of Earth Science, Environment and Resources, University of Naples Federico II, Naples, Italy

Correspondence
Vincenzo Allocca, Department of Earth Science, Environment and Resources, University of Naples Federico II, Naples, Italy.
Email: vincenzo.allocca@unina.it

Funding information
Ministry for Education, University and Research (MIUR, Italy)

Abstract

Groundwater bodies in the urbanized and densely populated aquifers or coastal floodplains may be subjected to groundwater rebound (GR), often causing serious risks of groundwater flooding (GF) to underground structures and infrastructures. This paper shows the results of a study carried out in the Naples' periurban area (Italy) to: investigate the dynamics and features of GR and GF phenomena, map flooded sites during 2013–2015 period, and provide an interpretative analysis of the factors that control the GF of private buildings and agricultural lands. At the municipality scale, since 1990 and until 2015, a remarkable and widespread GR was observed, with magnitude up to +16.54 m, triggering an unexpected GF of basements of buildings and agricultural soils. Field surveys proved that there is a time delay of the GF, ranging from 17 to 20 years, compared to the start of GR. Moreover, inhomogeneous distribution of flooding episodes is controlled by anthropogenic and natural factors. The obtained results are fundamental to design mitigation measures to GF hazard, and offer new perspectives to make Naples' periurban area more robust, smart and resilient against this new hydrogeological risk, undervalued by Italian legislation and local authorities.

KEYWORDS

aquifer mismanagement, groundwater flooding, groundwater rebound, land use change, urban hydrogeology

1 | INTRODUCTION

Urban transformations, climate changes, land use and groundwater use changes have caused groundwater levels rising (GWLr) phenomena worldwide. Indeed, GWLr has been observed in many areas of the world (Howard & Israfilov, 2002; Schirmer et al., 2013; Wilkinson, 1994) and it can be considered a current and global issue, as well as a relevant topic for the Urban Hydrogeology.

As it will be detailed in the next section, GWLr phenomena can have either natural or anthropogenic origins (e.g., Kreibich & Thieken, 2008) and, despite the variety of triggering mechanisms, they cause severe socioeconomic, environmental, and health impacts. Moreover, GWLr can occur at different spatial scales, from basin/large cities to individual sites, and it can feature different time frequencies, from occasional/seasonal to decadal occurring.

Among the main anthropogenic causes of the GWLr there is the reduction in the abstraction rate of

This is an open access article under the terms of the Creative Commons Attribution License, which permits use, distribution and reproduction in any medium, provided the original work is properly cited.
© 2021 The Authors. *Journal of Flood Risk Management* published by Chartered Institution of Water and Environmental Management and John Wiley & Sons Ltd.

groundwater temporally subsequent to a period of artificially low groundwater levels, these latter originated by high groundwater pumping or overexploitation. This triggering mechanism of the GWLr is named groundwater rebound (GR) (Crosta & De Caro, 2018). It is typical of urban centers and rural areas developing on unconfined aquifers, and is also observed in abandoned deep mine zones, where decline in anthropogenic activities and then the arrest or uncontrolled reduction of pumping groundwater allowed previous depressed groundwater levels to recover. GR can cause various negative effects such as the ground uplift and the deformation of aquifer systems (Chen et al., 2007; Yang et al., 2019). What is of utmost importance for the present study is that GR can be at the origin of groundwater flooding (GF) namely "*the emergence of groundwater at the ground surface away from perennial river channels or the rising of groundwater into the man-made ground, including basements of buildings and other subsurface infrastructure*" (Macdonald et al., 2008, 2012). GF phenomenon has either natural or anthropogenic origin, and its impacts can be severe on the environment, cultural heritage, utility activities, and human health, and can cause significant socioeconomic damages and costs (Azuma et al., 2014).

Among the major urban areas of the world affected by GR and GF phenomena, there is the Naples metropolitan area. In this mixed-land use area, since the early 1990s, a widespread GR phenomenon is in progress, caused by a drastic reduction (and sometimes interruption) of groundwater pumping from public and private wells. Focusing on this area, some studies based on literature data have analyzed GR phenomenon at the large scale (Allocca & Celico, 2008). Some more recent studies have analyzed GR-induced phenomena at the local scale, such as the ground uplift (Coda, Tessitore, et al., 2019; Coda, Confuorto, et al., 2019), and the variation of groundwater contamination (Coda, De Tommaso, et al., 2019). However, within Naples' periurban area, it is still missing a monitoring-based systematic analysis of the GR and GF phenomena; similarly, a mapping of flooded sites of structures and agricultural soils is still absent. This research aims to fill these gaps and advance the understanding of GR and GF phenomena occurring within Naples' periurban area at the municipality scale.

From a methodological point of view, thanks to intensive field monitoring, our paper contributes to an integrated vision of GR and GF processes, emphasizing the existence of a causal nexus between them. Precisely, a deep investigation of both GR and GF at an experimental site of the Naples metropolitan area is carried out, exploiting a unique and long-lasting hydrogeological dataset, as well as new hydrogeological monitoring and field surveys performed in the 2013–2015 period.

The study is focused on three main goals: (i) to develop a high-resolution 2D hydrostratigraphic and hydrogeological conceptual model of the pyroclastic-alluvial aquifer system, based on stratigraphic logs of 149 boreholes and 127 wells; (ii) to characterize, at the municipality scale, GR and GF phenomena, to improve knowledge about their spatiotemporal dynamics; and (iii) to map flooded sites during investigated period, by a citizen participatory approach, and analyze natural and anthropogenic factors that locally control GF of private buildings and agricultural lands.

This paper is structured as follows: Section 2 provides an overview of the literature as to GWLr and GF; Section 3 describes the geological, hydrographic and hydrogeological characteristics of the study area, as well as land use and groundwater environment changes; Section 4 shows the data and the methodological approach; Sections 5 and 6, respectively, comment the obtained results and provide their discussion, while Section 7 reports the concluding remarks.

2 | GWLR AND GF: AN OVERVIEW

As already pointed out, GR is only one of the possible typologies of GWLr. Albeit not always GR (and GWLr) engenders GF, recent literature has pointed out that among the many possible triggering mechanisms of GF, the one activated by GR is increasingly observed, as it will be documented below.

To begin with, GWLr has natural or anthropogenic origins (for the resume of case studies and references see Table S1 in supplementary materials), and the main natural causes listed in literature are: (i) increase of seawater level induced by climate change and glacial isostatic adjustment; (ii) natural consolidation of compressible sediment layers or bradysismic/volcano-tectonic land subsidence in coastal area, with consequent local sea-level increase; and (iii) seasonal variations of the rainwater infiltration and groundwater recharge by channel network, during and after heavy flash flood phenomena.

Conversely, the main anthropogenic causes of GWLr so far investigated in literature are: (i) artificially increased groundwater recharge in urban aquifers, caused by infiltration of imported water for domestic, irrigation and industrial consumption; (ii) artificially increased recharge caused by seepage from septic tanks systems, leakages from sewage systems, leaking water mains, over-irrigation of parks and gardens, irrigation return; (iii) underground constructions (e.g., tunnels, deep foundations, underground parks, subway stations, basements of buildings) in saturated zones of urban aquifers; (iv) anthropogenic land subsidence in coastal and

estuarine areas and consequent local sea-level rise; and (v) reduction of abstraction of groundwater (i.e., GR).

Based on Macdonald et al. (2008), Hughes et al. (2011), and Naughton et al. (2017), it is possible to start from the GF scenarios to classify them as having either natural or anthropogenic origin (Table S2 in supplementary materials). In the first group (natural origin), it is possible to list: (i) flooding in alluvial lowlands, as a response of unconfined and consolidated aquifers to extreme rainfall events; (ii) flooding in small alluvial flatlands, as a response of shallow aquifers with limited storage capacity and good hydraulic connection with river networks to intense rainfall; (iii) flooding in alluvial deposits, caused by groundwater by-passing or circumventing river channel flood defense structures; (iv) flooding in lowland karst systems, induced by ephemeral karst lakes (turloughs) and/or intense groundwater discharge via springs, resurgences or shallow, highly permeable horizons within the epikarst; and (v) flooding in coastal lowland areas, driven by sea-level rise under climate changes or during and following severe storms.

As to the GF triggered by anthropogenic causes, the list mainly includes: (i) flooding of underground structures creating barriers to groundwater flow and (ii) flooding of basements of buildings, and subsurface structures, infrastructures and underground cavities, induced by GR in urban centers and abandoned mine zones.

The above provided conceptualization of the existing scientific literature clearly points out that GWLr and GF are multidriven phenomena, widespread at global scale.

The analysis of the main natural and anthropogenic causes of GWLr and GF in different latitudinal and hydro-environmental contexts has contributed to implement the methodological approach of this research. Indeed, the present study is concerned with the last category in the lists of anthropogenic GWLr and GF phenomena just described, as observed within the large territory of the Naples' periurban area.

3 | DESCRIPTION OF THE STUDY AREA

3.1 | Geology and geomorphology

The study area, extended over about 14 km^2, corresponds to the municipalities of Casalnuovo di Napoli and Volla, located within the Naples metropolitan area (Italy).

From a geological point of view, the study area is located in the central-southern sector of the Campanian Plain (Figure 1(a)), a large alluvial plain formed in the Pliocene-Pleistocene by the filling of a regional semigraben structural depression, which was originated along the western side of the southern Apennines, during the opening of the Tyrrhenian Sea. Starting from 300k years (Rolandi et al., 2003), an intense volcanic activity occurred across the Campanian Plain with the formation of the Phlegraean Fields and Somma-Vesuvius volcanic districts. In the last 25k years, in addition to the deposition of volcaniclastic products, further sedimentation and erosional processes led to the filling of the structural depression by 1000–3000 m of alluvial, marine, and fluvio–palustrine sediments.

According to the updated geological data (ISPRA, 2019), four geological complexes have been identified in the study area (Figure 1(d)): Holocene pyroclastic–fluvial (PF) sediments; ash-fall pyroclastic deposits (P), dated 39.3–39.8k years; Holocene pyroclastic, alluvial-marine and palustrine (PAP) sediments as well as late Holocene volcanic and alluvial (VA) deposits. Furthermore, the northern and central-northern sectors are characterized by a tuff horizon, corresponding to the Campanian Ignimbrite (CI), in a zeolitized yellow facies, dated 39.28 $\pm$ 0.11k years (De Vivo et al., 2001). This tuff horizon does not crop out in the study area, being only recognizable in boreholes, with a thickness variable up to 40 m. Specifically, in the central-southern and southern sectors of the study area (Figure 1(d)), CI is absent due to erosion of paleo-Sebeto river and locally substituted by silt and clay deposits, as well as by lenses of peat and volcanic rocks (Bellucci et al., 1990).

From a morphostructural point of view (Figure 1(a,c)), the study area is subdivided between two catchment basin, Regi Lagni to the north, and the Sebeto River to the south, latter known as Volla river. The northern sector, crossed by Santo Spirito stream (Figure 1(c)) is part of the lowland floodplain of Regi Lagni, named the Acerra structural depression (Figure 1(a)). The southern sector, crossed by Cozzone and Volla rivers and Reale Lufrano channel, is lowland floodplain of subsiding tectonic depression, the Sebeto Valley (Figure 1(a)) set on Quaternary-active faults such as the buried deep Magnaghi-Sebeto fault. In these sectors, the landscape morphology is quite flat, with very gentle slopes, dipping up to 1%, and altitude varying from 25 to 12 m a.s.l., respectively. The two catchment basins are locally separated by a watershed divide, formed by the pyroclastic deposits of the Avellino plinian eruption (3780 year B.P.) of Somma-Vesuvius volcano (Rolandi et al., 1998), which crosses the central sector of the study area (Figure 1(c)), where the ground surface reaches altitudes up to 45 m a.s.l., and slopes up to 4%.

3.2 | Hydrography and hydrogeology

With the exception of the central sector, the large part of the study area is generally characterized by a shallow

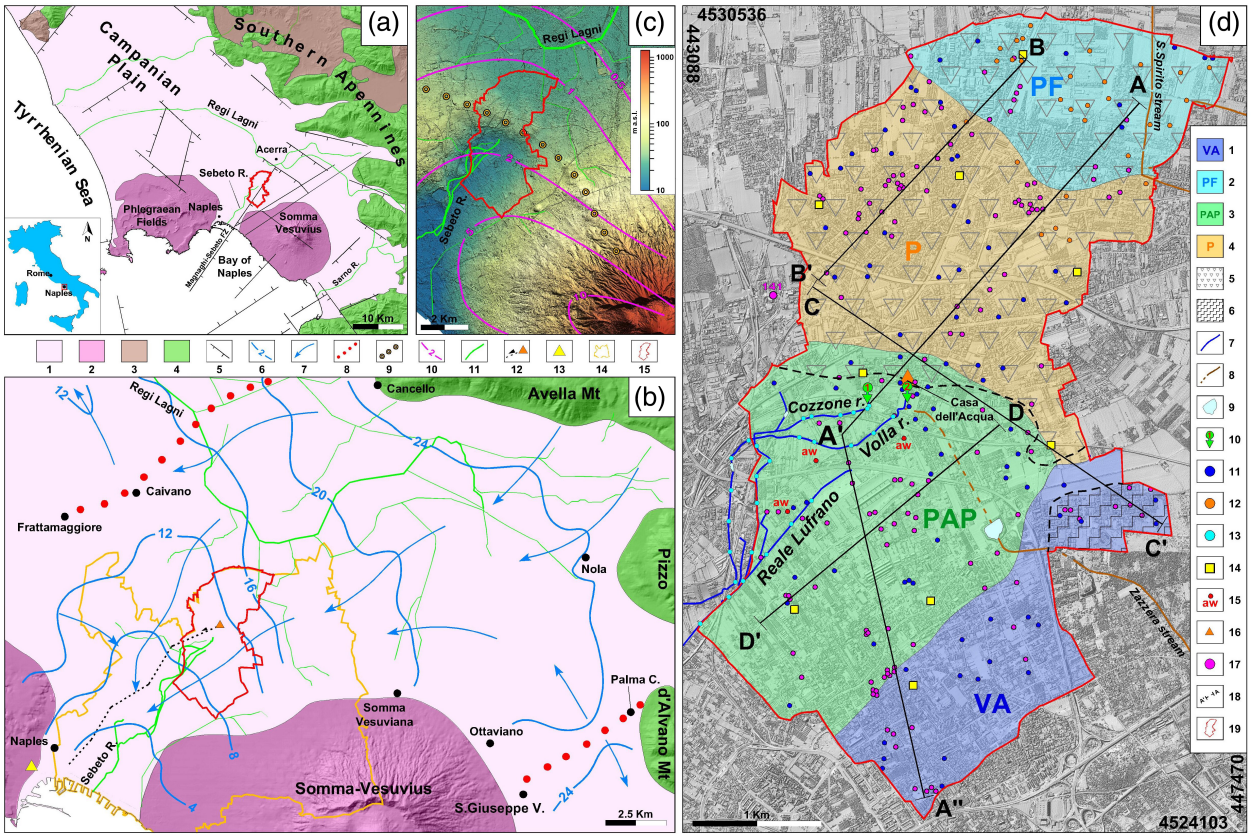

FIGURE 1 (a) Geological map of the Campanian Plain; (b) hydrogeological map of the eastern plain of Naples; (c) geomorphological setting of study area, and (d) hydrogeological setting of the study area. Legend of (a–c): 1) quaternary epiclastic deposits; 2) quaternary volcanic deposits; 3) Miocene deposits; 4) Mesozoic Apennine platform carbonates; 5) normal fault; 6) groundwater contour line relating to the 1994 year (m a.s.l.; Esposito, 1998, simplified); 7) groundwater flow direction; 8) groundwater divide; 9) watershed boundary; 10) isopach (thickness meters) of the ash-fall deposits of Avellino eruption (Rolandi et al., 1998); 11) hydrographic network system; 12) Bolla aqueduct; 13) San Marcellino Meteorological Observatory rain gauge (SMMO); 14) Naples and Volla swamps' reclamation consortium boundary; 15) study area. Legend of 1d): 1) VA complex; 2) PF complex; 3) PAP complex; 4) P complex; 5) sector with buried Campanian Ignimbrite (CI); 6) sector with buried lava rocks; 7) drainage network system; 8) urban drainage system (culverts); 9) tank septic system; 10) Cozzone (1) and Bolla (2) springs; 11) deep well; 12) shallow well; 13) river head monitoring point; 14) monitoring station; 15) artesian wells; 16) "Casa dell'Acqua" plant; 17) borehole; 18) cross-sectional lines; and 19) study area

water table and a drainage channel pattern which are typical of floodplain environments (Figure 1(b,d)). Historically, the main watercourse was the Sebeto river. Subsequently, during the Bourbon epoch (18th and 19th centuries), the hydrographic system of the Regi Lagni was artificially created: an ancient work of hydraulic reclamation, consisting of a network of channels dug to drain the ground and surface waters of marshy Acerra tectonic depression.

The central-southern sector of the study area shows typical morphological features of a swamp land, with a natural and artificial drainage micronetwork and some natural emersion of groundwater circulation, represented by the Bolla and Cozzone springs (Figure 1(d)), which were active until the beginning of the 20th century (Fiorelli, 1926). The Bolla spring, located close to the "Casa dell'Acqua," was tapped since the 4th century to feed the ancient homonymous aqueduct system serving the city of Naples (Figure 1(c,d)).

Due to its swampy features, the central-southern sector of the study area was interested by different hydraulic reclamation since 13th century and a complex natural and artificial drainage network was established to control surficial and groundwater drainage toward the Sebeto river. Other drainage works were carried out later on, since 1917, with the institution of the Naples and Volla swamps' reclamation Consortium, which is still active today (Figure 1(b)). However, during the last century the most significant reclaiming interventions were realized by farmers of the floodplain, who manually excavated microchannels to irrigate agricultural fields and to canalize groundwater and surface water (Caputo et al., 2000).

This drainage system, which was constantly maintained and managed, consisted of (Figure 2(e))

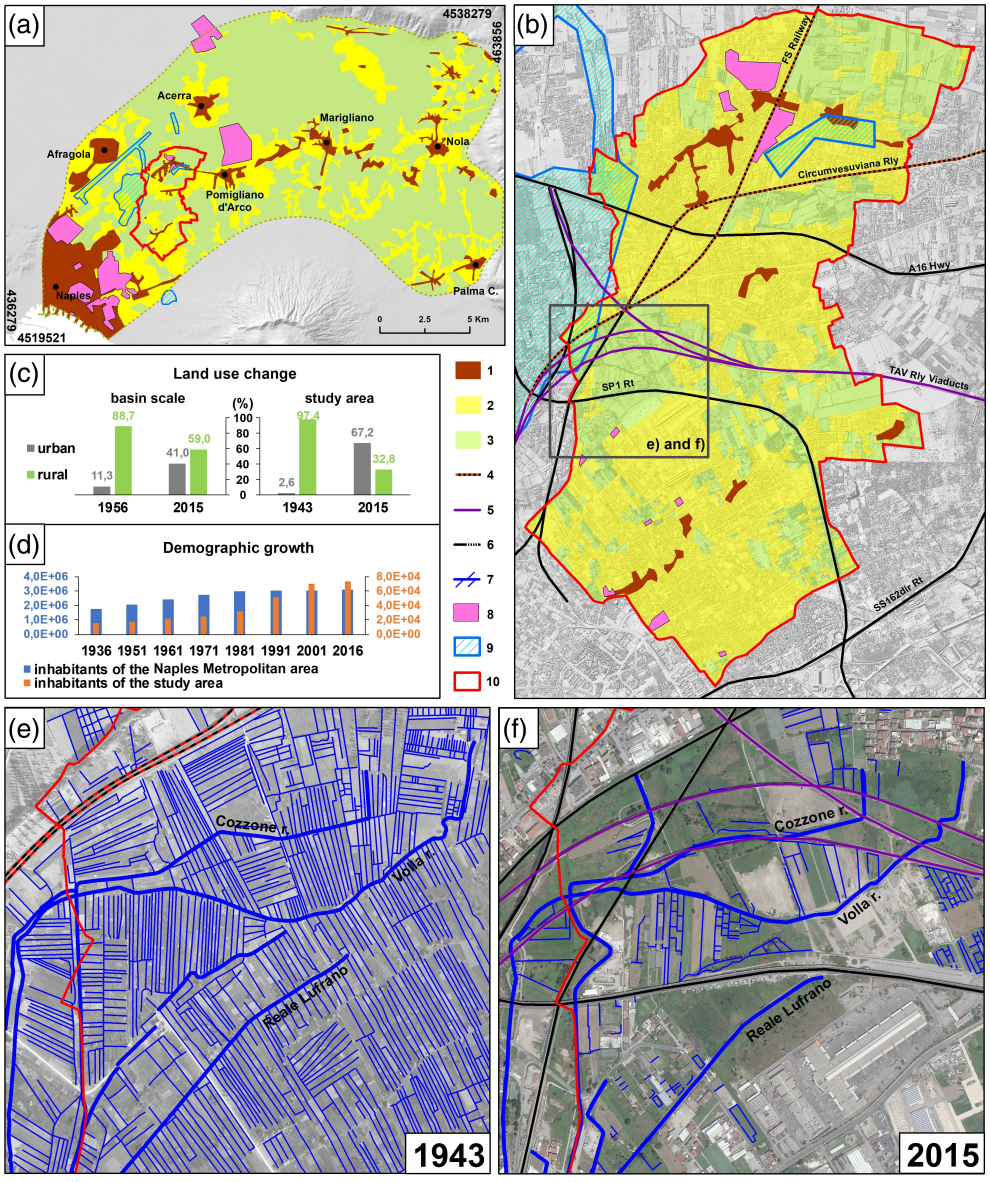

FIGURE 2 (a–c) Land use change and groundwater use change at the basin and local scale; (d) demographic growth for Naples metropolitan area and study area; (e) and (f) macro and micronetwork drainage system reconstructed for the 1943 (at the 1:25,000 scale) and 2015 years. 1) Urbanized area in the 1943–1956 period; 2) urbanized area in the 2015; 3) agricultural area in the 2015; 4) railway infrastructure constructed in the 1890–1910 period (Circumvesuviana rly and FS railway); 5) railway infrastructures constructed in the 1999–2007 period (TAV rly viaducts); 6) road infrastructures constructed in the 1955–1985 period (SP1 Rt, A16 Hwy, SS162dir Rt); 7) micronetwork drainage system; 8) dismissed industrial site in the 1995–2010 period; 9) Lufrano well field, partially decommissioned after the 1990; and 10) study area

longitudinal and transverse open ditches and furrows, that, by crossing and bordering the agricultural fields, created a micronetwork interconnected with the main rivers (Figure 2(e)). Furthermore, some farmers have always used an agronomic technique referred to as "baulatura" (Bazzoffi & Nieddu, 2011), characterized by a convex profile of ground surface, with slight slopes to facilitate water drainage laterally. Starting from the second half of the 20th century, the change of land use (Figure 2(a,b)) due to the quick and unplanned urbanization, industrialization, and infrastructuring have deeply changed the original aspect of rural territory of floodplain, modifying and canceling the ancient artificial drainage micronetwork system. Today, Volla and Cozzone rivers, Reale Lufrano channel, and Santo Spirito stream represent the local drainage system of groundwater and surface water (Figures 1(d) and 2(f)), and their hydraulic maintenance is entrusted to the Naples and Volla swamps' reclamation Consortium (Figure 1(b)).

From a hydrogeological point of view, the study area is a sector of the pyroclastic-alluvial plain of Naples (Figure 1(b)), where the groundwater circulation at basin scale can be considered unitary and interconnected with the Avella-Pizzo d'Alvano karst and Somma-Vesuvius volcanic aquifers (De Vita et al., 2018). At the local scale, the aquifer is characterized by a porous multilayered system, recharged by direct effective infiltration (which was estimated equal to about 300 mm/year by Allocca et al., 2014) and by groundwater flow coming from the upstream plain sector of the study area. Groundwater flow system is locally direct toward the Sebeto river and its tributaries (Figure 1(b)).

3.3 | Groundwater use and land use changes

The study area is one of the most densely populated urban areas of Italy, with nearly 75,000 inhabitants and a population density of about 5240 inhabitants/km^2 among highest in Europe. Until the '30s of the last century, floodplain groundwater was mainly used by inhabitants of rural villages for agriculture and local drinking needs, using shallow wells and manual methods for lifting groundwater, like the water-wheel or ancient Arabic system referred to as "noria," moved by power-animals. Since the post-World War II, floodplain groundwater has been intensively exploited for drinking water, agriculture and industry needs through modern pumping systems based on submerged pumps. The most important water-tapping public project was the Lufrano well field realized during 1930–1946, with about 156 wells distributed on an area of several square kilometers (Figure 2(a,b)), to meet water demand of the city of Naples. In the '70s and '90s of the last century, the Ponticelli and Acerra well fields were realized, respectively (Figure 2(b)), to provide drinking water to the hinterland of Naples. During this stage, a great number of unauthorized private wells for agricultural and industrial uses were realized with spatial density of 90–100 wells/km^2.

In the 1970–1989 period, an intensive use of groundwater resources by public and private wells occurred, causing a strong water balance disequilibrium and a groundwater overexploitation at the basin scale. Consequently, this disequilibrium determined a decline of piezometric levels and a deterioration of groundwater quality by the increase of nitrate, iron, manganese, and fluoride concentrations, exceeding the acceptable drinking water standards (Celico et al., 1997). Due to such a groundwater quality deterioration, Lufrano, Acerra, and Ponticelli well fields (Figure 2(a)) were partially or totally abandoned and groundwater withdrawals were drastically reduced (Figure 7). Since 1990s, private withdrawals for rural and industrial use have been drastically reduced, due to process of deindustrialization and land use change (Figure 2(b)). The land use changed strongly due to the continue and exponential population growth (Figure 2(d)), as well as the urban and economic development of Naples metropolitan area (Mazzeo, 2009; Salvati, 2014). At the basin scale, from 1956 to 2015, the urbanized zones increased from 11 to 41% of the total territory, while agricultural lands decreased from 88.7 to 59%. At the municipality scale, from 1943 to 2015, the urbanized zones increased from 2.6 to 67.2%, while rural areas declined from 97.4 to 32.8% (Figure 2(a,c)). Furthermore, in the 1995–2010 period, many industrial sites were dismissed and in the 1999–2007 period, three great railway viaducts of high-speed rail were constructed, with foundations characterized by deep piles with 1.20 m diameter and *length* up to about 41 m below the ground surface (Figure 2(b)).

4 | DATA AND METHODOLOGIES

4.1 | Hydrostratigraphic data

Using a LiDAR dataset (http://sit.cittametropolitana.na.it/lidar.html), a digital elevation model (DEM) of the study area, with 1 × 1 m cells, was implemented in a GIS environment and used for field surveys. A high-resolution 2D hydrostratigraphic model of the pyroclastic-alluvial aquifer system was reconstructed based upon a considerable geological and hydrogeological database consisting of: (i) deep stratigraphic data of wells available in literature (Coda, Tessitore, et al., 2019; Torrente et al., 2010), (ii) new geological maps and cartographic data at the 1:50,000 scale of Geological CARtography project (ISPRA, 2019), (iii) stratigraphic data of wells and boreholes available in the Geoportal of Italian Geological Survey (http://portalesgi.isprambiente.it/en), and (iv) borehole records archive of Casalnuovo di Napoli and Volla municipalities.

The geological and hydrogeological database is characterized by stratigraphic-lithologic logs of about 149 boreholes and 127 wells (Figure 1(c)), with an average density around 11.0 per km^2, and depths variable between 10 and 450 m below the ground level (Table 1). All wells and boreholes data collected were organized in a georeferenced database, to manage stratigraphic features and to recognize the different stratigraphic units, marker horizons, and lithofacies. For each borehole and well, a vertical log of hydraulic conductivity was obtained, assigning an average value for each lithofacies according to the Freeze and Cherry (1979), based on grain size and rocks types. This approach allowed to recognize the hydrogeological role of each lithofacies and geological formation, as aquifer, aquitard, or aquiclude.

Other information on geological and hydrogeological dataset used are summarized in Table 1.

4.2 | Hydrogeological data and drainage network density

From November 2013 to March 2015, a 6-month frequency hydrogeological monitoring of groundwater levels was carried out on 136 wells and piezometer and 28 river heads (Figure 1(d)), using a water level meter. Furthermore, since March 2015, a high frequency data acquisition system by nine monitoring stations with pressure

TABLE 1 Hydrogeological, meteorological, and stratigraphic dataset

Hydrogeological and meteorological data						
Monitoring period	**Type**	**Total number**	**Density (No/km^2)**	**Use**	**Depth range (m)**	**Reference**
August, 1924	Wells	85	6.07	A and D	4–12	Fiorelli (1926)
February–September, 1978	Wells	U.D.	U.D.	A, I, D, and D	U.D.	Celico (1983)
March, 1989	Wells	28	1.95	A, I, D, and D	10–60	Celico and De Paola (1992)
January, 1993	Wells	24	1.67	A, I, and D	10–70	Esposito (1998)
February, 1994	Wells	24	1.67	A, I, and D	10–70	Celico et al. (1995)
February, 2002	Wells	30	2.09	A, I, and D	10–70	Basin Authority of the North-Western Campania Region (2004)
November, 2013	Wells	127	9.07	A, I, and D	10–60	Field campaign
November, 2013	River heads	28	1.95	\	\	Field campaign
March, 2015	Wells	127	9.07	A, I, and D	10–60	Field campaign
March, 2015–ongoing	Piezometers	9	0.64	\	10–30	Field campaign
March, 2015	River heads	28	1.95	\	\	Field campaign
1924–2015 (annual rainfall) 2013–2015 (monthly rainfall)	Meteorological station	1	\	\	\	San Marcellino Meteorological Observatory (SMMO)
Stratigraphic data						
Monitoring period	**Type**	**Total number**	**Density (No/km^2)**	**Use**	**Depth range (m)**	**Reference**
1980–2015	Boreholes	148	10.34	Urban planning	10–60	Casalnuovo di Napoli and Volla municipalities unpublished database
\	Borehole	1	0.07	Scientific issues	430	Torrente et al. (2010)

Abbreviations: A, agricultural; D, drinking; I, industrial; U.D., unavailable data.

sensors and data loggers was installed and used to carry out slug tests. To characterize GR phenomenon, a temporal comparison between historical groundwater levels, new piezometric measurements, annual and monthly meteorological data, and groundwater pumping data was performed. To such a purpose, multitemporal maps of groundwater flow and maps of piezometric head variations were reconstructed by interpolation of piezometric levels (Table 1) using the triangulated irregular network method. Piezometric data of the whole dataset were plotted in temporal box-plot diagrams. Depth of water table maps was carried out for each period by subtracting the groundwater elevation raster from DEM. Finally, to analyze the modifications of the local micronetwork drainage system during the last century, and its possible influence on GF phenomenon, a temporal comparison between historical image of the 1943 of the Italian Military Geographic Institute (Figure 2(e)) and high resolution aerial photograph derived by 2015 satellite image (Figure 2(f)) was carried out, and for two periods the network drainage density was estimated.

All the cartographic products were elaborated in GIS environment using ESRI's ArcMAP software 10.1 version.

4.3 | Flood monitoring

From November 2013 to March 2015, a 6-month frequency monitoring and mapping of impacted agricultural soils and private building was carried out, using a citizen science approach. To map and detect the starting date and temporal recurrence of GF of private buildings and agricultural soils, local population received an online questionnaire sent by the local municipal administration. Subsequently,

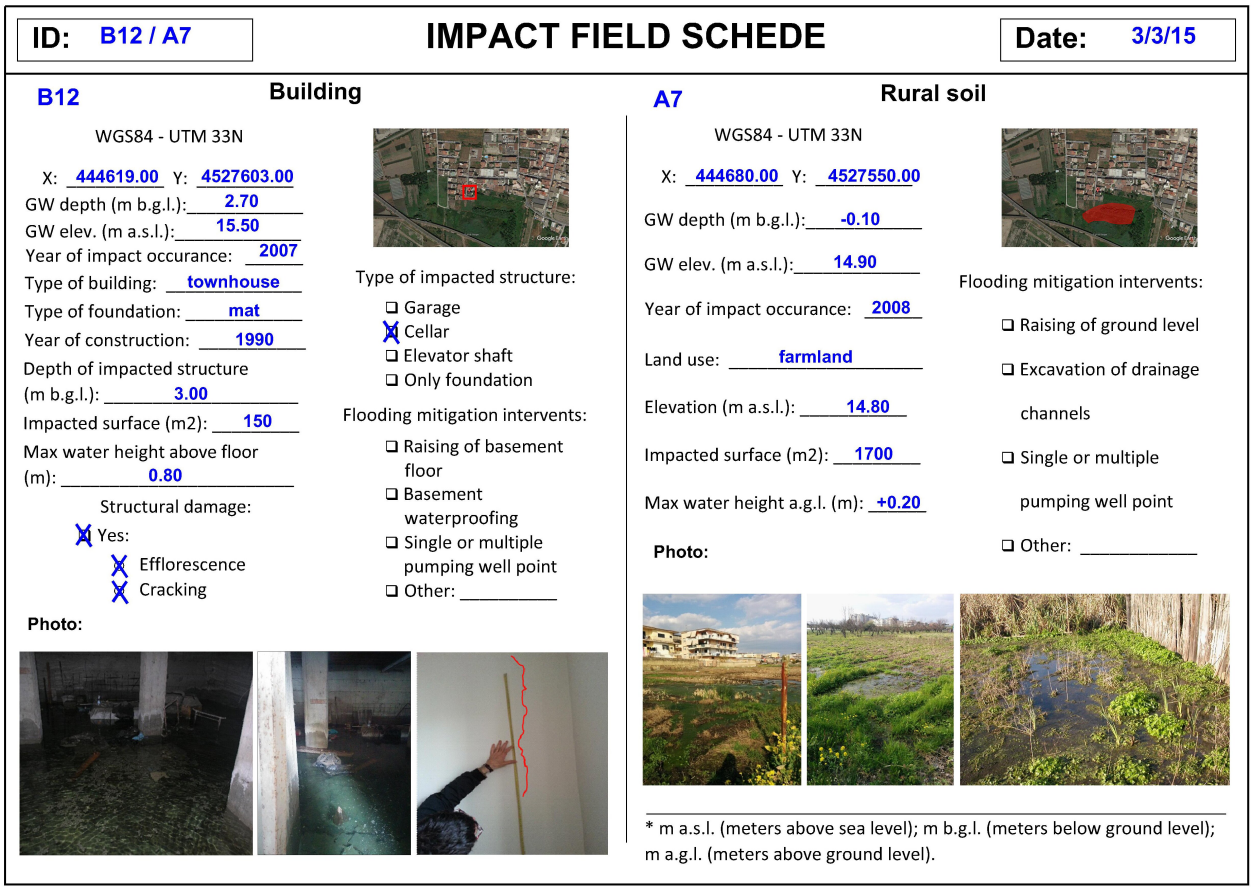

FIGURE 3 Field form for survey of flooded buildings and agricultural soils

for each flooded building registered through the online questionnaire, a number of parameters (coordinates, altitude, age and type of building, depth and type of foundation, depth of flooded underground facilities) were acquired, with the support of local cadastral municipality database and face-to-face interview with owners (Figure 3). In addition, temporal variations of water levels in the flooded structures, conditions of alteration and degradation and visual damage, as well as cracking pattern of structures were detected. For flooded agricultural lands, coordinates, altitude, and amplitudes about land parcel, as well as water levels above surface of flooded soils were measured. Moreover, type of active or passive protective measures aimed to flooding mitigation were detected. Finally, field data allowed to achieve multitemporal maps of GF of private buildings and agricultural soils, producing the first municipal GF GIS database.

5 | RESULTS

5.1 | Hydrogeological conceptual model

The 2D hydrostratigraphic model allowed, for the first time, to represent the geometry and architecture of the aquifer system down to about −400 m b.s.l., defining the top and bottom of two different aquifers. Figures 4 and 5 show a heterogeneous aquifer system, characterized by a multilayered discontinuous aquifer, which laterally evolves in a single aquifer. Starting from the northern sector (Figures 4 and 5(a,b)), an unconfined shallow aquifer, in the PF complex, and a deep semiconfined aquifer, in pyroclastic-alluvial deposits underlying CI horizon, occur. Both the aquifers have an average thickness of about 10 m and one 100 m, respectively, and they show small differences in terms of potential heads, although there are local variations of groundwater flow directions (Figures 4 and 5). The central sector is characterized by a single deep semiconfined aquifer in pyroclastic-alluvial deposits underlying the CI horizon. In the southern sector, where CI is absent, a single phreatic shallow aquifer is observed, locally characterized by artesian groundwater flow condition due to shallows aquicludes (lens of silts, clays, and peaty levels) within the PAP complex (Figure 4).

Figure 5(a,b) compares groundwater flow patterns of the deep and shallow aquifer system for November 2013 and March 2015, respectively. While Figure 5(d,e) shows groundwater flow scheme of the shallow unconfined aquifer for northern sector.

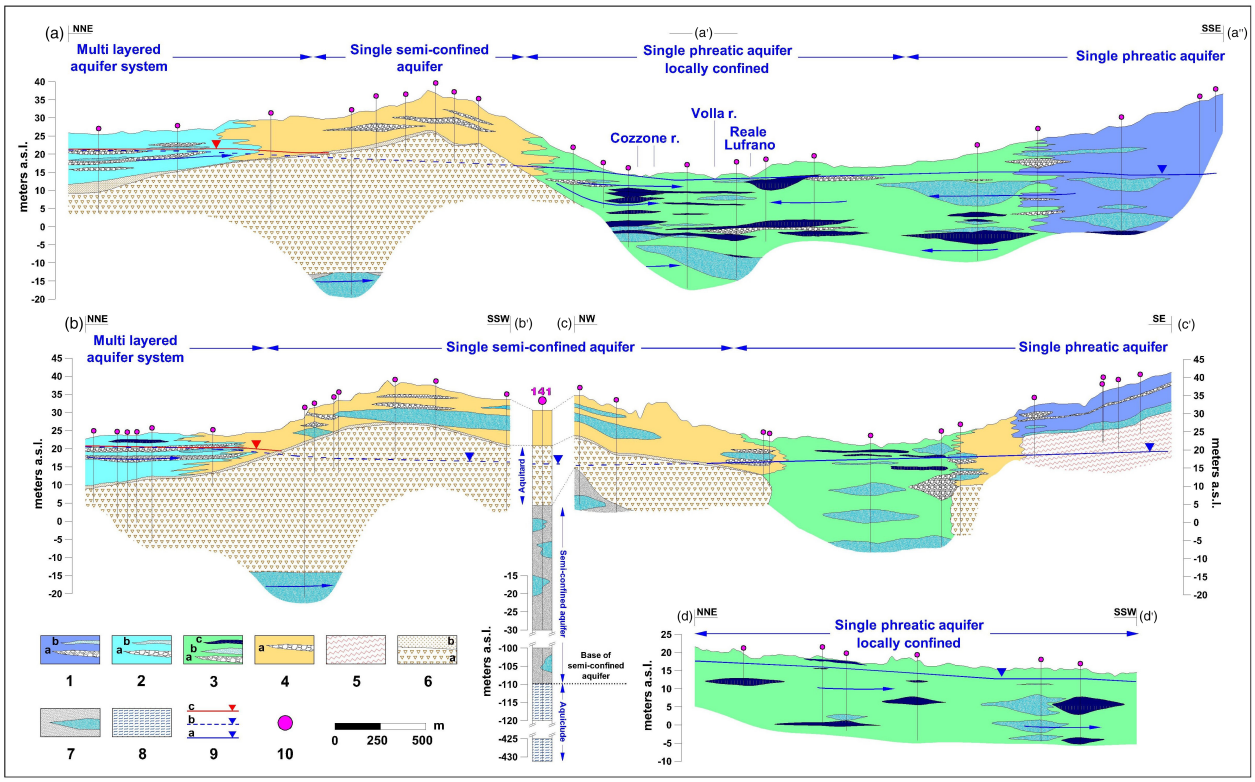

FIGURE 4 2D hydrostratigraphic model. 1) volcanic and alluvial (VA) complex (sandy silts) with interbedded: a) pumiceous lapilli horizons; b) sandy horizons; 2) pyroclastic–fluvial (PF) complex (sands, silts, and sandy silts) with interbedded: a) pumiceous lapilli horizons; b) sands e pumiceous lapilli horizons; 3) pyroclastic, alluvial-marine and palustrine (PAP) complex (sandy silts, silts, and clays) with interbedded: a) pumiceous lapilli horizons; b) sands, paleosols, and peat levels, c) marshy clay-sands and clay-silts; 4) P complex (silty sands) with interbedded: a) pumiceous-scoriaceus lapilli horizons; 5) Somma-Vesuvius lavas; 6) Lithoid (a) and incoherent (b) CI; 7) deep semiconfined pyroclastic-alluvial aquifer (silty sands and sands); 8) basal aquiclude (marine clays); 9) phreatic (a) and semiconfined (b) piezometric level of the deep aquifer, and phreatic level of shallow aquifer (c); and 10) borehole

For the deep semiconfined aquifer, in the northern and central sectors (Figure 5(a,b)) groundwater flow is about NE–SW, thus being consistent with groundwater scheme at basin scale. In the southern sector, the groundwater flow direction is mainly E-W, converging toward Cozzone and Volla rivers and Reale Lufrano channel, which locally are physically continuous with groundwater flow and behaving as gaining streams.

For the shallow unconfined aquifer of northern sector (Figure 5(d,e)), groundwater circulation is oriented toward N and S, bypassing thus the IC top, and Santo Spirito stream feeds only partially the underlying shallow aquifer, as the concrete stream bed is positioned at a level higher than the water table. For the shallow aquifer, the hydraulic gradient varies between 5.9×10^{-4} and 2.0×10^{-2}, whereas for the deeper water table it varies between 8.7×10^{-4} and 4.3×10^{-2}.

For the 2013–2015 period, temporal variations of groundwater levels for both aquifers are shown in Figure 5(c,f). Both water table levels display a generalized rise, with a magnitude variable at the municipality scale. For the deeper aquifer (Figure 5(c)), the highest magnitude amounts to 2.44 m, and was recorded in the northern-western sector of the study area, whereas low values, smaller than 0.10 m, were observed in the south-western sector, near the Cozzone and Volla rivers and Reale Lufrano channel, having the latter a fixed piezometric heads. For the shallow unconfined aquifer (Figure 5(f)), the highest magnitude amounting to 1.54 m was recorded in the northern-eastern sector of the study area.

Finally, in Figure 5(g) monthly rainfall trend is shown. Downward trend in the time series suggests that the rise of piezometric levels measured between 2013 and 2015 is not related to a change in the groundwater recharge rate.

5.2 | GR characterization

Figure 6(a,b) shows groundwater elevation (m a.s.l.) and groundwater depth (m b.g.s.) for eight hydrodynamic

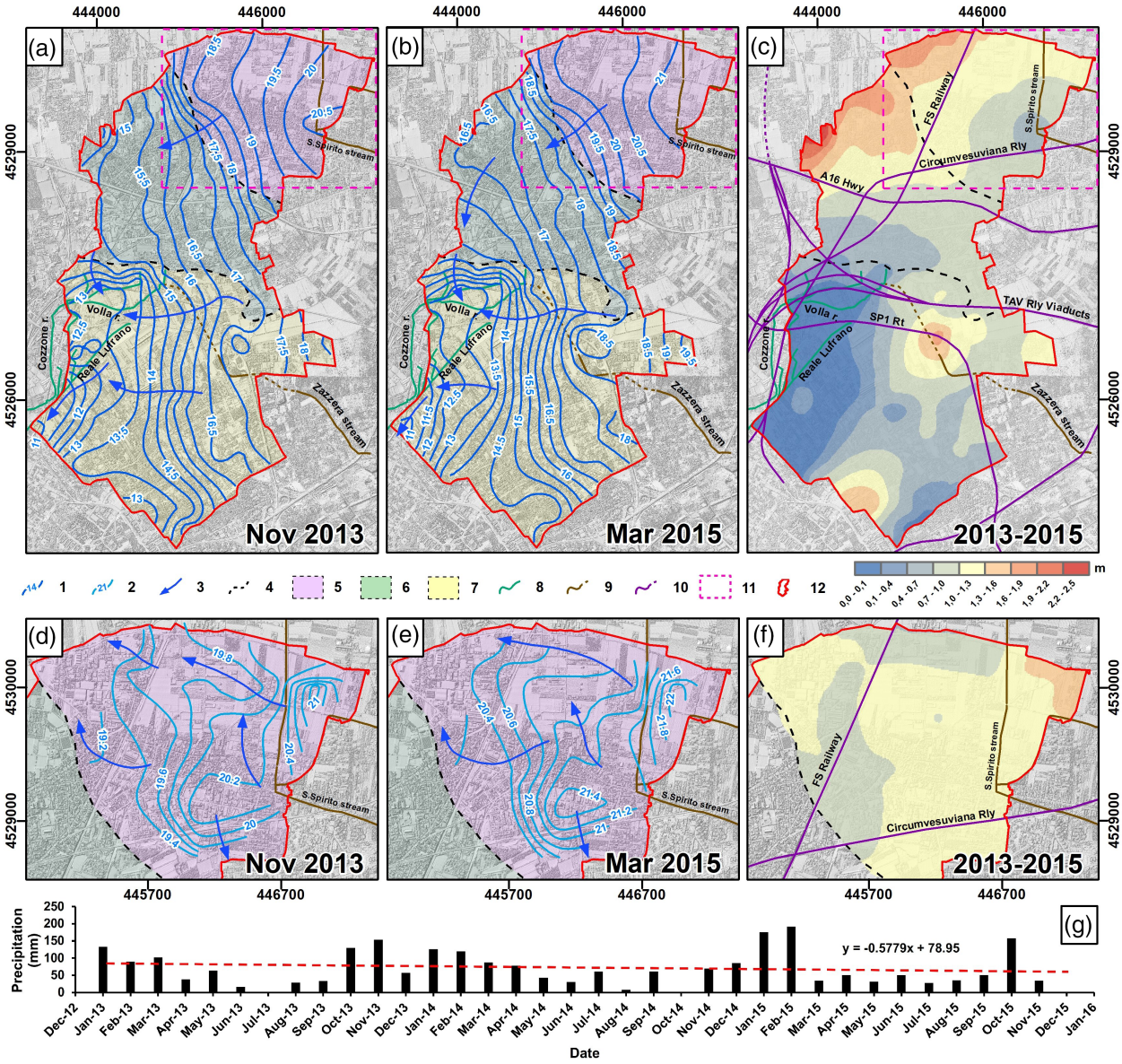

FIGURE 5 Groundwater flow pattern of the deep and shallow aquifer, for the period (a and d) November 2013, (b and e) March 2015, and piezometric head variations between these measurement periods (c and f). (g) San Marcellino Meteorological Observatory rain gauge (SMMO') monthly rainfall. 1) Piezometric contour line of the deep aquifer (m a.s.l.); 2) piezometric contour line of the shallow aquifer (m a. s.l.); 3) groundwater flow direction; 4) aquifer type boundary; 5) sector with shallow and deep aquifer; 6) sector with deep semiconfined aquifer; 7) sector with phreatic aquifer, locally confined; 8) surface and groundwater drainage network; 9) urban drainage system (culverts) and concrete channels; 10) railway infrastructures constructed in the 1999–2007 period; 11) box of Figure 5(d–f); and 12) study area

scenarios, respectively, each representative of the hydrogeological history of the aquifer system from 1924 to 2015. Here, the attention is focused on three scenarios, because they are particularly significant in explaining the groundwater level evolution and indicative of two subsequent hydrogeological phases (1924–1989 and 1989–2015), which were characterized by declining and rising groundwater levels, respectively.

The first one is the 1924 scenario, indicative of a hydrogeological equilibrium for the aquifer system. Groundwater was used for local agriculture and drinking needs for villages habitants, by shallow wells and manual abstraction methods. Water table levels vary from 22.45 to 9.68 m a.s.l., equal to 34.01 and 0–0.50 m b.g.s. The second one is the 1989 scenario, representative of a groundwater overexploitation period. Intense groundwater pumping (about 4.2 m^3/s for drinking use, see Figure 7(b)) by numerous public and private deep wells caused a considerable water budget deficit (Allocca & Celico, 2008) and piezometric levels depletion up to −2.06 m b.s.l., equal to 42.47 m b.g.s. The third one is the 2015 scenario, representative of present-day hydrogeological conditions, in which

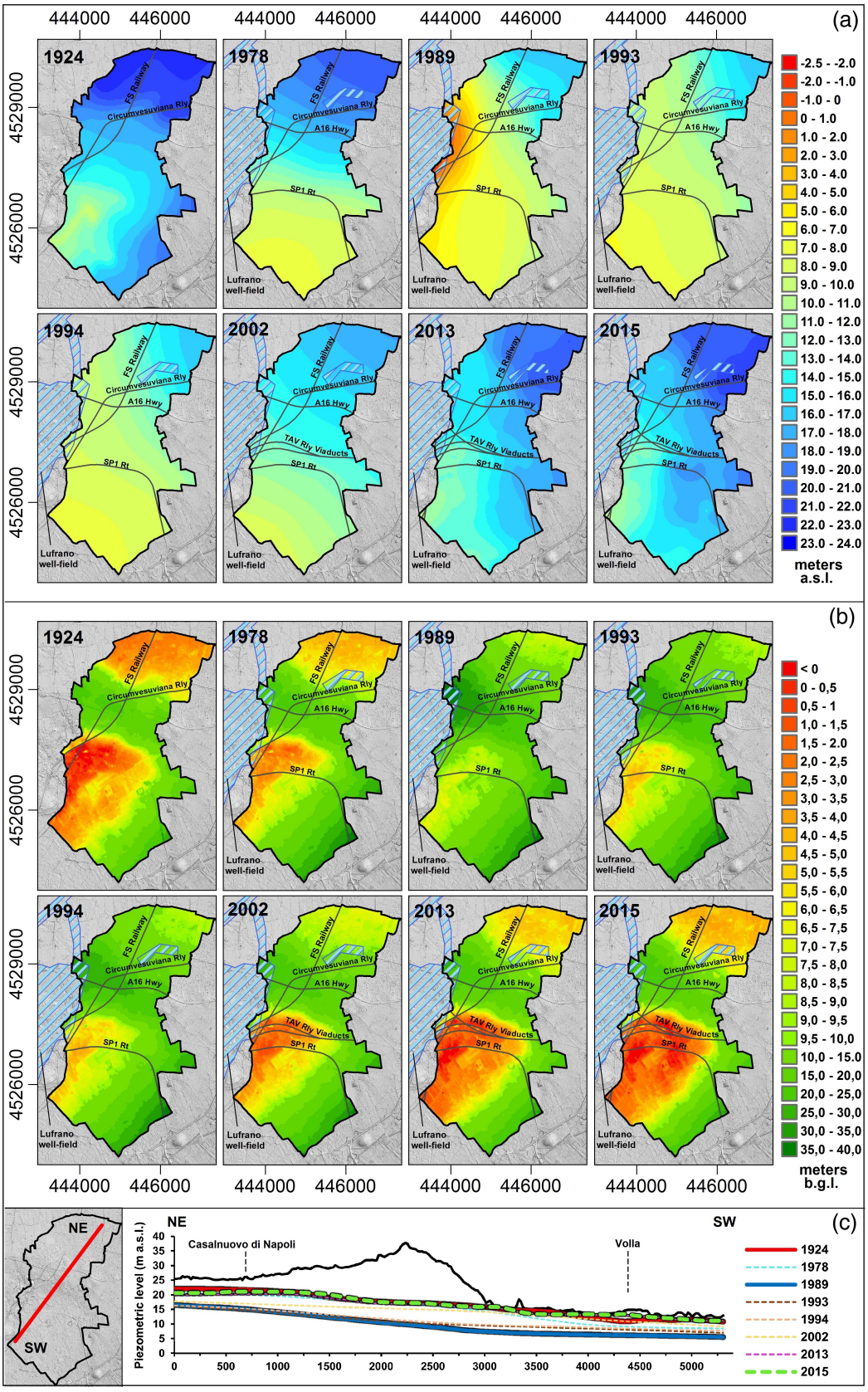

FIGURE 6 Hydrodynamic scenarios in the period 1924–2015, in terms of (a) piezometric heads (m a.s.l.), (b) depth of water table (m b.g.l.) and (c) piezometric profiles (m a.s.l.)

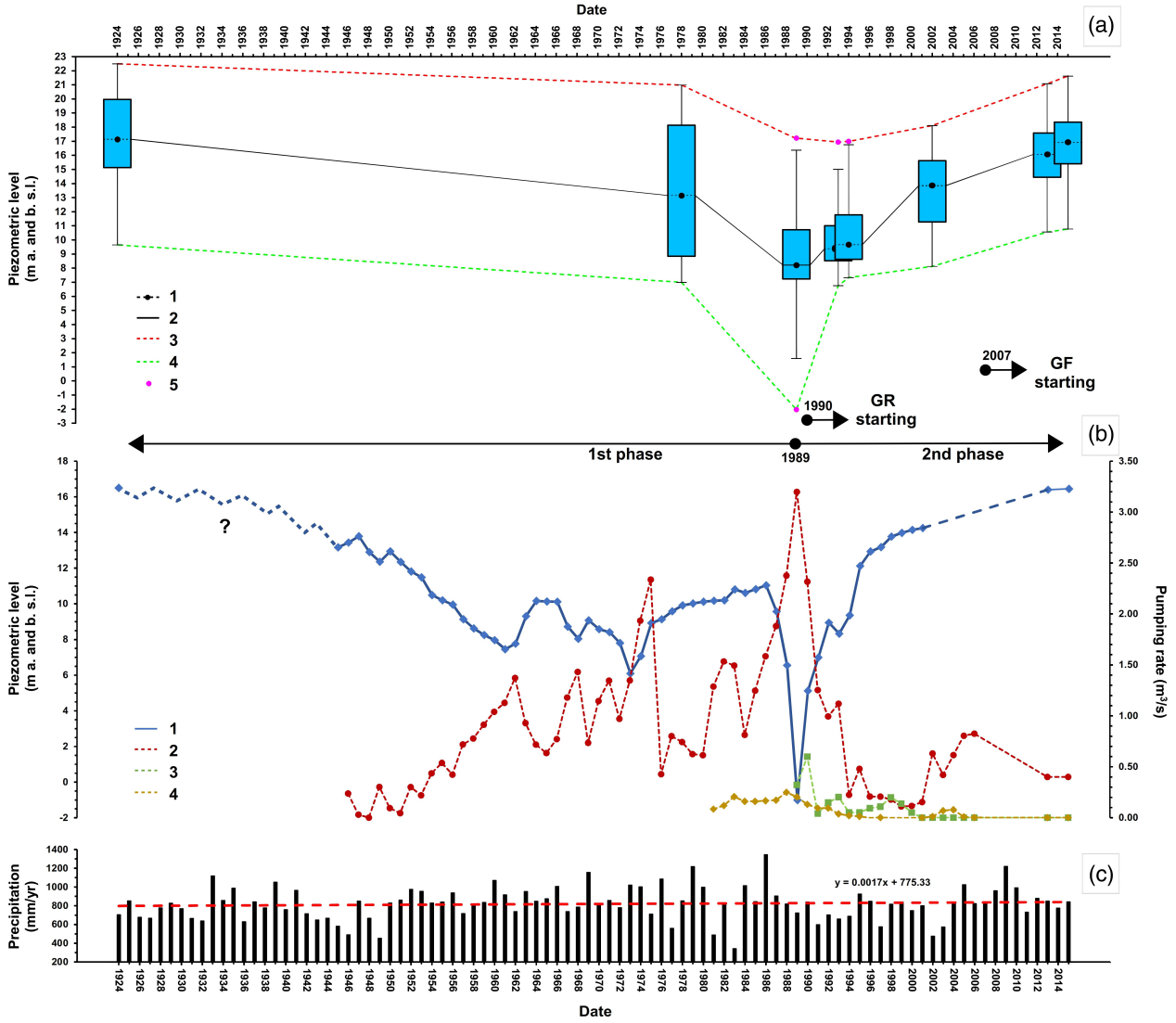

FIGURE 7 (a) Box plots of piezometric levels (m a. and b. s.l.) in the study area; (b) piezometric levels (m a. and b. s.l.) and withdrawals (m^3/s) in Lufrano, Acerra, and Ponticelli well fields; (c) San Marcellino Meteorological Observatory rain gauge (SMMO') annual rainfall. Legend a): 1) median piezometric head; 2) median trend; 3) maximum trend; 4) minimum trend; 5) outliers; legend c): Time series of: 1) piezometric levels Lufrano well-field; 2) Lufrano well-field withdrawal; 3) Acerra well-field withdrawal; 4) Ponticelli well-field withdrawal

aquifer system has almost recovered 1924 hydrogeological equilibrium due to strong reduction of groundwater pumping. Piezometric level increased up to 21.58 and 10.53 m a.s.l., equal to 36.49 and 0–0.50 m b.g.s.

In Figure 6(c), the three scenarios are highlighted as piezometric profiles along a NE–SW oriented section to show the vertical lowering and raising of the water table in the study area.

In the box plot of Figure 7(a), the temporal trends of piezometric levels are reported. Each trend shows that the GR phenomenon has started in 1990 and is widespread in the whole study area, with a magnitude up to maximum of 16.54 m. In agreement with Coda, Tessitore, et al. (2019), the 1990–2015 period was characterized by two subperiods, each one with different magnitude and rising velocity of the GR (Table 2). The 1990–2002 subperiod is characterized by a mean magnitude of about 4.10 m (up to a maximum of 14.43 m) and a mean velocity of 0.32 m/year (up to a maximum value of 1.11 m/year). In the 2002–2015 subperiod, a reduction of the magnitude is observed, with mean values of about 3.49 m (up to a maximum of 6.51 m), and a mean velocity of about 0.27 m/year (up to a maximum of 0.50 m/year). The remarkable variability of the GR is strongly dependent on the distance from the abandoned Lufrano well field (Figures 2(b) and 6), considered as the hypocenter of the piezometric deformation induced by Lufrano pumping, and observed at the local and basin scale. Therefore, the highest magnitude of piezometric rise is observed (Table 2) in the central-western sector of study

TABLE 2 Magnitude (m) and rising velocity (m/year) during GR period (1990–2015)

	Magnitude (m)			Rising velocity (m/year)		
Period and subperiod of the GR	**Minimum**	**Mean**	**Maximum**	**Minimum**	**Mean**	**Maximum**
Period 1990–2015	3.50	7.88	16.54	0.13	0.30	0.64
Subperiod 1990–2002	0.47	4.10	14.43	0.04	0.32	1.11
Subperiod 2002–2015	0.29	3.49	6.51	0.02	0.27	0.50

Abbreviation: GR, groundwater rebound.

area, in correspondence of the eastern boundary of Lufrano well field, as this sector is closer to the area of the well field.

Moreover, the comparison between the time series of groundwater levels, withdrawals (Figure 7(b)) and annual rainfall (Figure 7(c)) confirms that climate-induced changes have not played a significant role on GR at the decadal scale, in agreement with the downward sloping trend in the mean annual precipitation index observed at the regional scale (De Vita et al., 2012). Finally, data suggest that a not significant role on GR was played by deep foundations of railway viaducts constructed in the 1999–2007 period, since the rising groundwater levels were recorded both upstream and downstream of these civil engineering works (Figures 2(b), 5(c), and 6(b)).

5.3 | GF features

Data from the online questionnaire, field surveys and mapping display that GF phenomena affect private buildings and agricultural lands. By contrast, there are no public structures, infrastructures, and cultural resources impacted by GF, as occurs in other sectors of the Naples metropolitan area (Allocca et al., 2018; Stellato et al., 2020).

In the study area, the early episodes of GF affecting private buildings and agricultural lands were recorded, respectively, in 2007 and 2010, with a time delay variable from 17 to 20 years in comparison to the beginning of the GR, started in 1990. In a "cause-effect" perspective, the GF episodes observed are the consequence of piezometric levels rise induced by the cessation in groundwater pumping for public and private use. However, unlike the GR process, widely distributed at the municipality scale (Figures 5 and 6), the GF phenomenon shows a sectorialized pattern, with a distribution spatially and temporally inhomogeneous, as a typical leopard spots-shape (Figures 8 and 10). Indeed, the private buildings and agricultural soils affected by flooding are only located

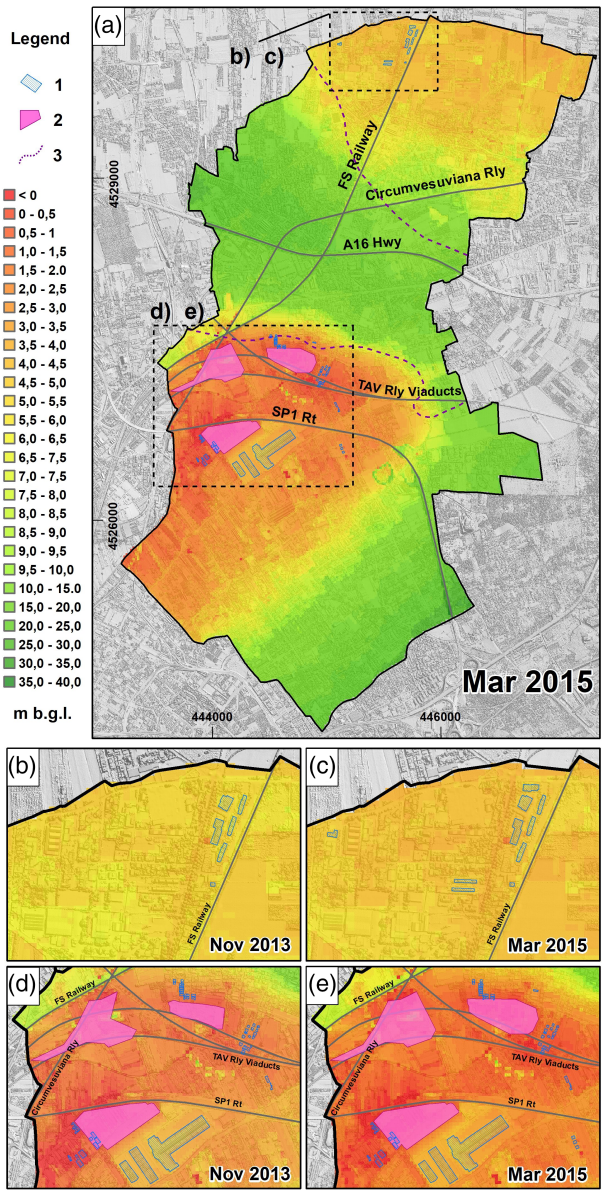

FIGURE 8 Maps of the groundwater depth (m b.g.l.) in the deep (a, d, and e) and in the shallow aquifer (b and c), and spatiotemporal distribution of groundwater flooding (GF) episodes in the period November 2013–March 2015. 1) Flooded buildings; 2) flooded agricultural soils; and 3) boundary of aquifers reported in Figure 5

in the northern and southern sectors of the study area. In particular, in the northern sector, only few private buildings (Figure 8(b,c)) are impacted by shallow unconfined water table, with flooding episodes of garages, cellars, and lift shafts. Conversely, no flooded agricultural lands were detected in this sector. Moreover, collected field data by citizen's survey shows that these private buildings were constructed in the 1990–2000 period, when groundwater levels of the aquifer system, affected by groundwater pumping for drinking, industrial and agricultural use (Figures 2(b) and 6), were locally characterized by depth variable between about 9 and 6 m from ground surface (Figure 6(b)).

Similarly, in the southern sector, only few private buildings (Figure 8(d,e)) reveal flooded underground structures (garages and cellars) and flooded ground-floors of private buildings. These underground structures were constructed in the 1985–1995 period, when stressed piezometric levels by pumping for drinking, industrial and agricultural use, were locally characterized by depth about 6 m below ground surface (Figure 6(b)). In addition, in this sector, unlike the northern one, some agricultural lands are affected by flooding episodes, with local outcropping of the shallow water table (Figure 8(d, e)) near drainage channels of Cozzone, Volla, and Lufrano rivers.

In Table 3, the temporal variability of GF phenomenon observed at the municipality scale is shown. In 2013, a total number of 44 private buildings have been flooded (with a total buildings surface equal to 61,898 m^2), among which 6 are located in the northern sector, and 38 in the southern sector (Figure 8(b,d)). In 2015, flooded buildings increased to 52 (with a total area of flooded buildings of about 66,000 m^2), among which 10 are located in the northern sector and 42 in the southern sector (Figure 8(c,e)). From 2013 to 2015, the number of private buildings and surface of agricultural soils flooded has increased of about 15 and 20%, respectively (Table 3).

The inhomogeneous spatial distribution of GF episodes observed during the monitoring period is linked to the local hydrostratigraphic and geomorphological characteristics of aquifer system. In the northern sector, the shallow aquifer hosted within the PF complex is very flat (Figure 1(d)) and it is characterized by unconfined groundwater flow, with a water table oscillating between 3.5 and 5.7 m below surface. Consequently, the private buildings with underground structures (garages, cellars, and lift shafts), located at a depth greater than 3.5 m from surface, are constantly flooded, with greater impact in the winter period, during intense and prolonged rains that recharge the shallow pyroclastic-alluvial aquifer.

In the central sector, where the P complex outcrops (Figure 1(d)), the aquifer is characterized by a single deep semiconfined aquifer in pyroclastic-alluvial deposits underlying the CI horizon (Figures 4 and 5). Despite the presence of numerous private and public buildings with underground structures (garage, cellars, and ancient underground cavities dug into the tuff horizon) located at depths up to 15–20 m from ground surface, in this sector there are not GF phenomena, because the aquifer is locally characterized by a semiconfined groundwater flow (Figures 4 and 5).

In the southern sector, the complex floodplain aquifer hosted within the PAP complex (Figure 1(d)) is phreatic, with a shallow water table oscillating between 0.0 and 1.5 m below soil surface. Consequently, the private buildings with underground structures (garages, cellars, and lift shafts) located at depth greater than 1.5 m from ground surface, are constantly flooded, especially during the recharge phase of the shallow floodplain aquifer. The unconfined groundwater table morphology is controlled by floodplain hydrographic network, driving groundwater flow toward Cozzone, Volla, and Reale Lufrano rivers (Figure 5(a,b)). At the local scale, artesian flow conditions are caused by the presence of discontinuous lenses of low permeability of silts, clays and peaty horizons within the PAP complex.

Moreover, the map of spatial distribution of GF episodes, observed during the monitoring period, shows that, with respect to the local groundwater flow (Figure 5(a–c)), the impacted private buildings and agricultural lands are located upstream and downstream of civil engineering structures (Figures 8 and 10). Consequently, the "barrier effect" of the impervious deep foundation on the groundwater flow, that in some cases may occur (Attard et al., 2016), is absent or negligible in the

TABLE 3 Number and area of buildings and agricultural soils affect by GF in the 2013–2015 period

	Private buildings		Agricultural soils
Period	**No.**	**Area (m^2)**	**Area (ha)**
November 2013	44	61898.16	20.60
March 2015	52	65916.85	25.36
Δ (2015–2013)	8 (+15.38%)	4018.68 (+6.10%)	4.76 (+19.77%)

Abbreviation: GF, groundwater flooding.

study area at the municipality scale. Therefore, field evidences show that a not significant role, in terms of triggering causes of GR and GF dynamics, was played by deep foundations of the three great railway viaducts of high-speed rail constructed in the 1999–2007 period (Figures 6 and 8). The time variability of GF, that is, the increase in the number of buildings and the extension of the flooded ground surface between 2013 and 2015 period, is attributable to the fact that GWLr was in progress during the monitoring period (Figures 5(c,f) and 7(b)).

As shown in Figure 9, GF phenomena is causing tangible and intangible damages: (i) on private buildings and its facilities (garages, cellars, and lift shafts) due to the structural deformations (vertical and horizontal cracks), groundwater infiltration and deterioration of foundations and pillars (Figure 9(a–h)) and (ii) on rural environment, because of the scarce healthiness of the flooded territory and total loss of agricultural soils (Figure 9(i–n)). Moreover, among possible socioeconomic impacts of the above described damages, it is possible to envisage loss in the local estate market, due to drop of buildings and rural soils prices, but also consequences for the health of flooded populations, due to poor conditions in terms of environmental hygiene in water-damaged buildings.

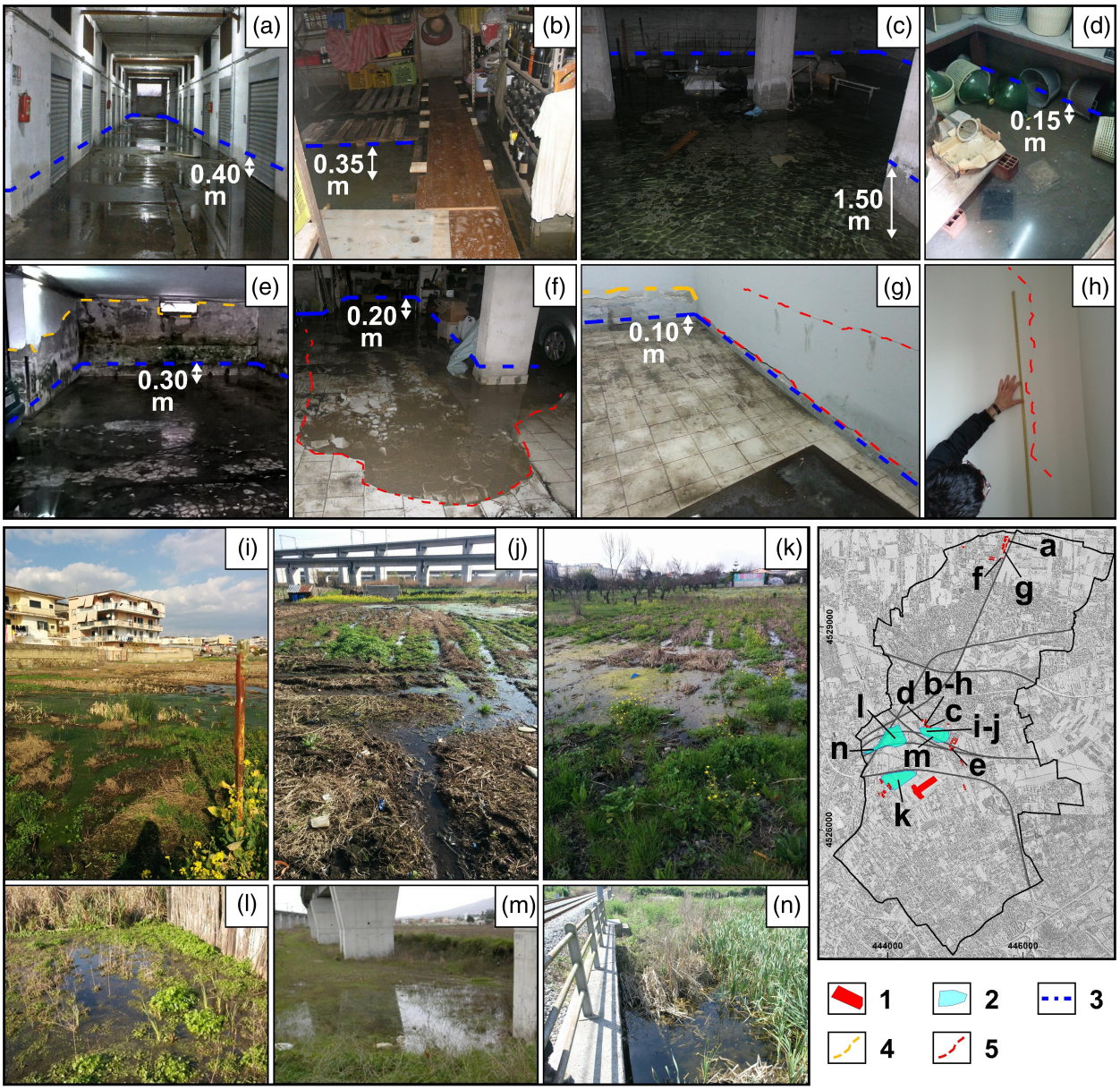

FIGURE 9 Damages on buildings and agricultural soils. 1) Flooded buildings; 2) flooded agricultural soils; 3) maximum height reached by piezometric level; 4) height reached by efflorescence and deterioration of pillars and walls; and 5) vertical and horizontal cracks

6 | DISCUSSION

The floodplain aquifer of the study area, although relatively small in terms of extension, shows significant heterogeneity in the geometry of the aquifer and groundwater flow.

By comparing the map of groundwater level rise with the one of GF, it is recognizable an apparent mismatch between the location of flooded sites and rate of rising groundwater levels (Figure 10(a–c)).

For the northern sector, the flooded private buildings are located away from Santo Spirito stream (Figure 10 (b)), in an area where the unconfined shallow aquifer is characterized by a medium rate of rising piezometric levels, ranging from 0.7 to 1.3 m, and a flat surface morphology, with slopes less than 1%. In the same sector, the deep semiconfined aquifer (Figure 10(a)) does not impact private buildings, although it is characterized by of groundwater rise up to 2.5 m.

For the southern sector, the flooded private buildings and agricultural soils are located near Cozzone, Volla, and Reale Lufrano drainage channels, where the unconfined shallow aquifer is characterized by a low rate of rising groundwater levels, ranging from 0.1 to 0.4 m (Figure 10(c)), and land morphology is flat, with slopes less than 1%.

The heterogeneities in the geometry and structure of flood plain aquifer, and the hydrogeomorphological and anthropogenic factors acting at the local scale help to explain the inhomogeneous distribution of the GF episodes, with a typical leopard spots-shape, that certainly is not random. Based on field evidence, a hydrogeologically based interpretation of the GF phenomenon has been proposed, highlighting the natural and anthropogenic factors that locally control the GF spatial distribution of private buildings and agricultural soils. Among the anthropogenic factors facilitating GF it is possible to quote: (i) an erroneous design of private buildings, built in the period 1985–2000, performed with nonwaterproofed underground structures deeper than current groundwater levels (see Figure 11(a)); (ii) the total disappearance of the ancient agricultural drainage micronetwork system due to urbanization, infrastructuring, and abandonment of agricultural lands, as it is well recognizable from the strong downsizing of the local drainage density from 45.1 to 8.7 km/km^2 (Figure 11(c)); and (iii) the loss of hydraulic efficiency of the main drainage system of Cozzone, Volla e Reale Lufrano river, due to the poor maintenance state of channels and total occlusion by spontaneous vegetation (Figure 11(c)) that locally causes a water flow blockage effect.

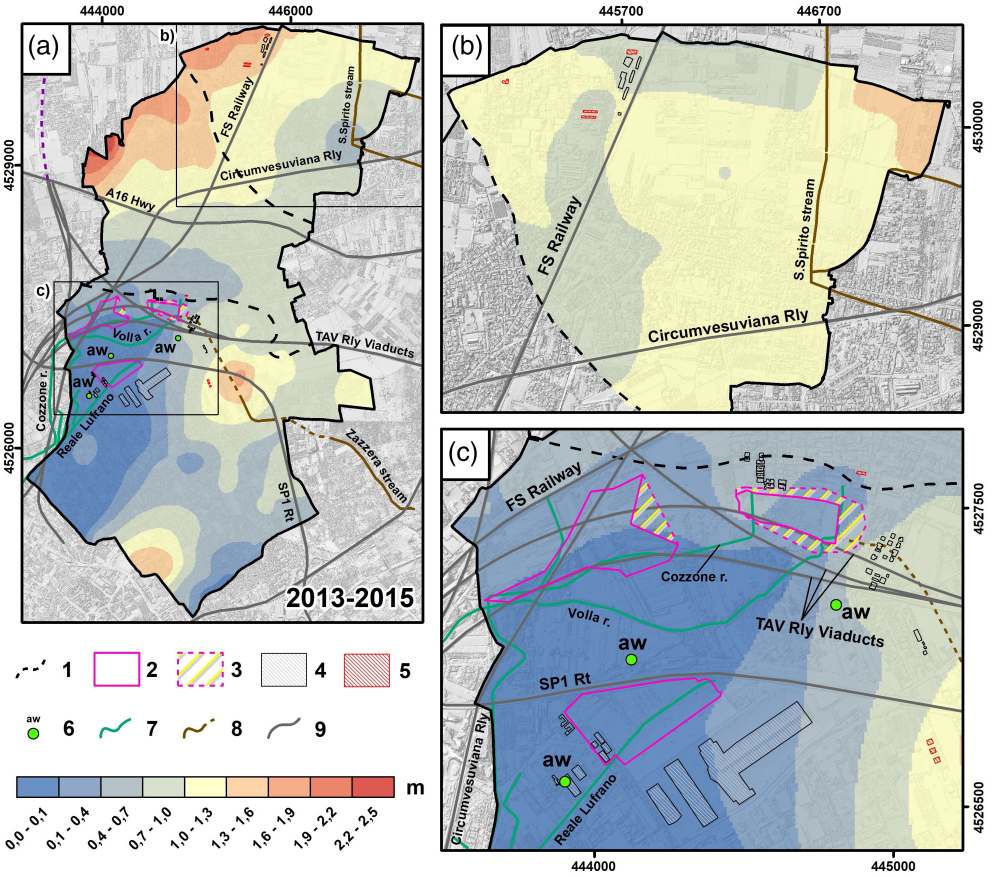

FIGURE 10 Comparison between piezometric head variations in the period November 2013–March 2015 for the shallow and deep semiconfined aquifer (a) and shallow unconfined aquifer (b) and (c), and spatiotemporal distribution of groundwater flooding (GF) in the northern (b) and southern (c) impacted sectors. 1) Aquifer type boundary; 2) 2013′ flooded agricultural soils; 3) 2015′ increment of flooded agricultural soils; 4) 2013′ flooded private buildings; 5) 2015′ increment of flooded private buildings; 6) artesian well; 7) surface and groundwater drainage network; 8) urban drainage system (culverts); and 9) linear infrastructure

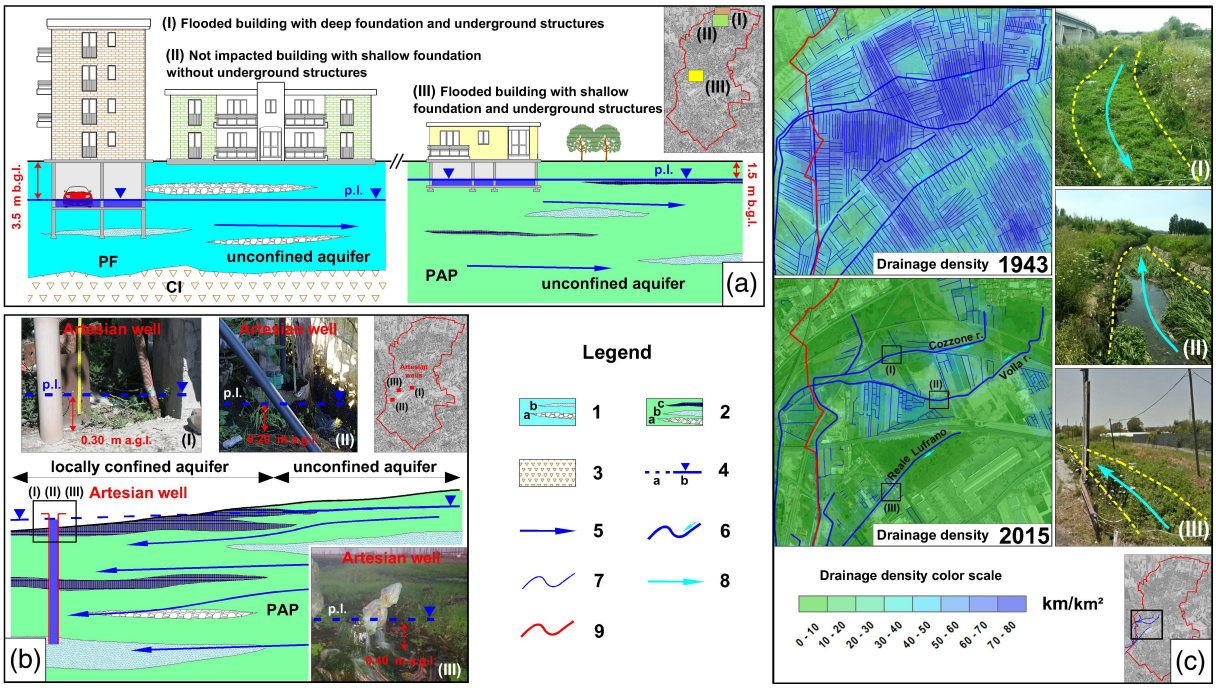

FIGURE 11 Anthropogenic and natural factors controlling groundwater flooding (GF). (a) Impacted private buildings, nonimpacted private buildings and piezometric thresholds depth (in red color) to consider in the future underground structures design; (b) local and permanent conditions of artesian groundwater levels around nonflooded soils; (c) drainage density modification of network system from 1943 to 2015 (Figure 2e,f), occlusion of channels by spontaneous vegetation and water flow blockage effect. 1) PF complex; 2) PAP complex, 3) CI tuff horizon; 4) confined (a) and unconfined (b) piezometric levels (red number in the box a): Maximum piezometric level p.l. (m b.g.l.); 5) groundwater flow direction; 6) surface and groundwater drainage macro-network system; 7) agrarian drainage micronetwork system; 8) surface water flow direction; and 9) study area

As to the natural factors, lithology and structure of the aquifer have a key control on GF, shaping the spatial distribution of GF according to the presence of a shallow phreatic water table and thickness of unsaturated zone.

In the northern sector of the study area, the interaction between the anthropogenic facilitating factors and thickness of unsaturated zone lower than 4 m has been observed to be associated with GF of private buildings.

In the southern sector, where GF has involved buildings and agricultural soils, a thickness of unsaturated zone lower 1.5 m has been observed to be associated to GF of private buildings (Figure 11(a)). Differently, the presence of low permeability shallow lenses (silts and/or peat lenses), that locally cause permanent artesian conditions of groundwater (up to +0.20 ÷ 0.40 m a.g.s.), is a mitigating factor for GF of soils, as observed in some not flooded soils (Figure 11(b)) characterized by the presence of artesian wells; similar evidences has been observed in other alluvial aquifers including lowland and upland floodplains (Cloutier et al., 2014; O' Dochartaigh et al., 2019).

The findings here discussed innovate the existing literature by providing new evidences for the study area, based on an intensive effort in data monitoring, that has never been undertaken in previous literature. This allows a better understanding of the triggering mechanisms and anthropogenic/natural factors that locally control GF of private building and agricultural lands in Naples' periurban area. Moreover, the hydrogeological monitoring has allowed to define two safe piezometric thresholds for both sector impacted. These piezometric thresholds, amounting to about 3.5 m and 1.5 m b.g.s., for northern and southern sectors, respectively (Figure 11(a)), correspond to maximum thickness of the unsaturated medium to be considered in future designs of underground structures, in order to prevent interactions with groundwater and floodings for nonwaterproofed buildings.

7 | CONCLUSIONS

In an experimental site of the Naples' periurban area, spatial–temporal evolution and the features of GR phenomenon were analyzed and characterized by using historical hydrogeological data starting from 1924 and hydrogeological monitoring of 136 wells and piezometers in the 2013–2015 period. Moreover, using the information collected through an ad hoc citizen survey and those

from field survey on private buildings and agricultural soils, the GF phenomenon induced by GR was mapped, creating the first flooding inventory map at the municipal scale.

By the field investigations and monitoring, the following findings and major conclusions were obtained:

- starting from second half of the 20th century and until 1989, an extraordinary modification of groundwater flow pattern was observed, due to mismanagement and overexploitation of the pyroclastic-alluvial aquifer system, causing groundwater levels depletion, up to −2.06 m b.s.l.;
- from 1990 to 2015, a remarkable and widespread GR phenomenon was recorded, with values up to +16.54 m, triggering an unexpected GF of agricultural soils and private buildings constructed in the 1985–2000 period;
- the early GF episodes started in 2007 and 2010 for private buildings and agricultural soils, respectively, indicating a considerable time delay variable from 17 to 20 years, in comparison to the beginning of GR process;
- despite GR measured from 1990 to 2015 encompasses the entire study area, with different magnitudes and velocity, the GF phenomenon occurs only in the northern and southern sectors, showing a typical leopard spots-shape and an inhomogeneous distribution as it is locally controlled by anthropogenic and natural factors;
- for both sectors impacted, a safeguard piezometric threshold have been identified to consider in future for new underground structures designs, in order to avoid direct interactions with water table or flooding of non-waterproofed structures;
- at the municipality scale, a not significant role on GR and GF phenomena was played by annual and monthly precipitation variations and deep foundations of railway infrastructures constructed in the 1999–2007 period in the study area.

These findings were not reported and discussed by previous studies because of the absence of monitoring data, and allow a better understanding of mechanisms and anthropogenic/natural factors that locally control GF phenomena.

The methodological approaches used to characterize GR and GF phenomena in the Naples' periurban area can be applicable and exportable to other urban and rural environments in southern Italy, as well as to other Italian floodplains and cities, that are currently experiencing similar urban groundwater problems. The obtained results are important to identify structural and nonstructural measures aimed at increasing urban resilience and enhancing safety of local communities, and to develop GF susceptibility maps (e.g., Allocca et al., 2021), as new tools for the prevention of the risk and correct urbanization planning in the Naples metropolitan area.

ACKNOWLEDGMENTS

The authors wish to thank the technical Department of municipalities of Casalnuovo di Napoli and Volla, for the technical support during the research program. The research was undertaken and funded within Research Agreement "*Studio delle dinamiche idrogeologiche delle falde di Casalnuovo di Napoli (Napoli)*" (Scientific Coordinator: V. Allocca; Scientific Director: P. De Vita) signed in July 2013 (*Prot. 2013/0079737 del 13/09/2013*). This research was also supported by the PRIN Project (2017) Prot. 2017HPJLPW "*URGENT – Urban Geology and Geohazards*: *Engineering geology for safer*, *resilieNt and smart ciTies*" funded by the Ministry for Education, University and Research (MIUR, Italy). Finally, the authors greatly acknowledge the four anonymous reviewers, the associate editor and the editor in chief Dr Paul Samuels for their precious suggestions and comments which improved the quality of the final version of the manuscript.

DATA AVAILABILITY STATEMENT

Data available on request from the authors.

ORCID

Vincenzo Allocca https://orcid.org/0000-0001-7146-2438

REFERENCES

Allocca, V., & Celico, P. (2008). Scenari idrodinamici nella piana ad Oriente di Napoli (Italia) nell'ultimo secolo: Cause e problematiche idrogeologiche connesse. *Giornale di Geologia Applicata*, *9*(2), 175–198.

Allocca, V., Coda, S., De Vita, P., Di Rienzo, B., Ferrara, L., Giarra, A., Mangoni, O., Stellato, L., Trifuoggi, M., & Arienzo, M. (2018). Hydrogeological and hydrogeochemical study of a volcanic-sedimentary coastal aquifer in the archaeological site of Cumae (Phlegraean Fields, southern Italy). *Journal of Geochemical Exploration*, *185*, 105–115.

Allocca, V., Di Napoli, M., Coda, S., Carotenuto, F., Calcaterra, D., Di Martire, D., & De Vita, P. (2021). A novel methodology for groundwater flooding susceptibility assessment through machine learning techniques in a mixed-land use aquifer. *Science of the Total Environment*, *790*(2021), 148067.

Allocca, V., Manna, F., & De Vita, P. (2014). Estimating annual groundwater recharge coefficient for karst aquifers of the southern Apennines (Italy). *Hydrology and Earth System Sciences*, *18*, 803–817.

Attard, G., Winiarski, T., Rossier, Y., & Eisenlohr, L. (2016). Review: Impact of underground structures on the flow of urban groundwater. *Hydrogeology Journal*, *24*, 5–19.

Azuma, K., Ikeda, K., Kagi, N., Yanagi, U., Hasegawa, K., & Osawa, H. (2014). Effects of water-damaged homes after flooding: Health status of the residents and the environmental risk factors. *International Journal of Environmental Health Research*, *24*(2), 158–175.

Basin Authority of the North-Western Campania Region. (2004). *Il contributo al Piano di Tutela delle Acque della Regione Campania*. Grafica Montese snc. ed.

Bazzoffi, P., & Nieddu, S. (2011). Effects of waterlogging on the soil structure of some Italian soils in relation to the GAEC cross-compliance standard maintenance of farm channel networks and field convexity. *Italian Journal of Agronomy*, *6*(s1), e9.

Bellucci, F., Corniello, A., De Riso, R., & Russo, D. (1990). Idrogeologia della Piana a NE di Napoli. *Memorie della Società Geologica Italiana*, *45*, 339–349.

Caputo, V., Navarro, A., Storia, V., & Tarantino, O. (2000). *Le paludi della "Civitas Neapolis": l'opera della bonifica nella trasformazione idrogeologica-urbanistica-antropica*. Associazione Onlus Casali.

Celico, F., Celico, P., Esposito, L., Guadagno, F. M., Habetswallner, F., & Mele, R. (1995). Sull'evoluzione idrogeologica dell'area del Sebeto (Campania). *Geologia Applicata e Idrogeologia*, *30*, 567–581.

Celico, P. (1983). Idrogeologia dei massicci carbonatici, delle piane quaternarie e delle aree vulcaniche dell'Italia centro-meridionale: Marche e Lazio meridionali, Abruzzo, Molise e Campania Quaderni della Cassa per il Mezzogiorno, 4/2, 1–225, Roma.

Celico, P. & De Paola, P. (1992). La falda dell'area napoletana: ipotesi sui meccanismi naturali di protezione e sulle modalità di inquinamento. Atti Giornata di Studio "Acque per Uso Potabile"; CI ESSE I Centro Scientifico Internazionale: Milan, Italy 387C–412C.

Celico, P., Esposito, L., & Guadagno, F. M. (1997). Sulla qualità delle acque sotterranee nell'acquifero del settore orientale della Piana Campana. *Geologia Tecnica e Ambientale*, *4*, 17–27.

Chen, C. T., Hu, J. C., Lu, C. Y., Lee, J. C., & Chan, Y. C. (2007). Thirty-year land elevation change from subsidence to uplift following the termination of groundwater pumping and its geological implications in the metropolitan Taipei Basin, northern Taiwan. *Engineering Geology*, *95*, 30–47.

Coda, S., Confuorto, P., De Vita, P., Di Martire, D., & Allocca, V. (2019). Uplift evidences related to the recession of groundwater abstraction in a pyroclastic-alluvial aquifer of southern Italy. *Geosciences*, *9*, 215.

Coda, S., De Tommaso, G., Iuliano, M., Jantáková, N., Villani, R., & Allocca, V. (2019). Variation of groundwater contamination related to groundwater rebound in the eastern plain of Naples. Proceedings of the XI Convegno Nazionale Dei Giovani Ricercatori in Geologia Applicata. 19-21 September 2019, Matera (Italy).

Coda, S., Tessitore, S., Di Martire, D., Calcaterra, D., De Vita, P., & Allocca, V. (2019). Coupled ground uplift and groundwater rebound in the metropolitan city of Naples (southern Italy). *Journal of Hydrology*, *569*, 470–482.

Cloutier, C-A., Buffin-Bélanger, T., Larocque, M. (2014). Controls of groundwater floodwave propagation in a gravelly floodplain. *Journal of Hydrology*, *511*, 423–431.

Crosta, G. B., & De Caro, M. (2018). Groundwater rebound. In P. Bobrowsky & B. Marker (Eds.), *Encyclopedia of engineering geology*. Encyclopedia of earth sciences series. Springer.

De Vita, P., Allocca, V., Celico, F., Fabbrocino, S., Mattia, C., Monacelli, G., Musilli, I., Piscopo, V., Scalise, A. R., & Summa, G. (2018). Hydrogeology of continental southern Italy. *Journal of Maps*, *14*, 230–241.

De Vita, P., Allocca, V., Manna, F., & Fabbrocino, S. (2012). Coupled decadal variability of the North Atlantic oscillation, regional rainfall and karst spring discharges in the Campania region (southern Italy). *Hydrology and Earth System Sciences*, *16*, 1389–1399.

De Vivo, B., Rolandi, G., Gans, P. B., Calvert, A., Bohrson, W. A., Spera, F. J., & Belkin, H. E. (2001). New constraints on the pyroclastic eruptive history of the Campanian volcanic plain (Italy). *Mineralogy and Petrology*, *73*, 47–65.

Esposito, L. (1998). Nuove conoscenze sulle caratteristiche idrogeochimiche della falda ad Oriente della città di Napoli (Campania). Quaderni di Geologia Applicata, 5–1/98, Pitagora Editrice, Bologna.

Fiorelli, T. (1926). Cenni sull'andamento della falda acquifera nel sottosuolo della zona tra Napoli e Pomigliano d'Arco in relazione colla costituzione geologica e la topografia e idrologia superficiale del territorio medesimo. Annuali del Genio Civile, Fascicolo VII, 613-626, Roma.

Freeze, R. A., & Cherry, J. A. (1979). *Groundwater*. Prentice-Hall.

Howard, K. W. F., & Israfilov, R. G. (2002). Current Problems of Hydrogeology in Urban Areas, Urban Agglomerates and Industrial Centres. NATO Science Series. 4, Earth and Environmental Sciences, 8, 1-500, Kluwer Academic Pub, Springer.

Hughes, A. G., Vounaki, T., Peach, D. W., Ireson, A. M., Jackson, C. R., Butler, A. P., Bloomfield, J. P., Finch, J., & Wheater, H. S. (2011). Flood risk from groundwater: Examples from a chalk catchment in southern England: Flood risk from groundwater. *Journal of Flood Risk Management*, *4*(3), 143–155.

ISPRA. (2019). Geological maps of Italy, scale 1:50.000, Sheets No. 446-447 and No. 448. Retrieved from http://www.isprambiente.gov.it/Media/carg/campania.html

Kreibich, H., & Thieken, A. H. (2008). Assessment of damage caused by high groundwater inundation. *Water Resources Research*, *44*(9), W09409.

Macdonald, D., Dixon, A., Newell, A., & Hallaways, A. (2012). Groundwater flooding within an urbanised flood plain. *Journal of Flood Risk Management*, *5*, 68–80.

Macdonald, D. M. J., Bloomfield, J. P., Hughes, A. G., Macdonald, A. M., Adams, B., & McKenzie, A. A. (2008). Improving the understanding of the risk from groundwater flooding in the UK, in: FLOODrisk 2008, European Conference on Flood Risk Management, Oxford, UK. CRC Press, The Netherlands.

Mazzeo, G. (2009). Naples. *Cities*, *26*, 363–376.

Naughton, O., McCormack, T., Gill, L., & Johnston, P. (2017). Groundwater flood hazards and mechanisms in lowland karst terrains. In *Advances in karst research: Theory, fieldwork and applications* (Vol. 466, pp. 397–410). Geological Society, London, Special Publications.

Ó Dochartaigh, B. É., Archer, N. A. L., Peskett, L., MacDonald, A. M., Black, A. R., Auton, C. A., Merritt, J. E., Gooddy, D. C., & Bonell, M. (2019). Geological structure as a control on floodplain groundwater dynamics. *Hydrogeology Journal*, *27*, 703–716.

Rolandi, G., Bellucci, F., Heizler, M. T., Belkin, H. E., & De Vivo, B. (2003). Tectonic controls on the genesis of ignimbrites from the

Campanian volcanic zone, southern Italy. *Mineralogy and Petrology*, *79*, 3–31.

Rolandi, G., Petrosino, P., & Mc Geehin, J. (1998). The interplinian activity at Somma–Vesuvius in the last 3500 years. *Journal of Volcanology and Geothermal Research*, *82*, 19–52.

Salvati, L. (2014). Population distribution and urban growth in southern Italy, 1871–2011: Emergent polycentrism or path-dependent monocentricity? *Urban Geography*, *35*, 440–453.

Schirmer, M., Leschik, S., & Musolff, A. (2013). Current research in urban hydrogeology—A review. *Advances in Water Resources*, *51*(2013), 280–291.

Stellato, L., Coda, S., Arienzo, M., De Vita, P., Di Rienzo, B., D'Onofrio, A., Ferrara, L., Marzaioli, F., Trifuoggi, M., & Allocca, V. (2020). Natural and anthropogenic groundwater contamination in a coastal volcanic-sedimentary aquifer: The case of the archaeological site of Cumae (Phlegraean fields, southern Italy). *Water*, *2020*(12), 3463.

Torrente, M. M., Milia, A., Bellucci, F., & Rolandi, G. (2010). Extensional tectonics in the Campania volcanic zone (eastern Tyrrhenian Sea, Italy): New insights into the relationship between faulting and ignimbrite eruptions. *Italian Journal of Geosciences*, *129*(2), 297–315.

Wilkinson, W. B. (1994). Groundwater problems in urban areas. Proceedings of the International Conference organised by the Institution of Civil Engineers and held in London, 2–3 June 1993. Thomas Telford, London.

Yang, J., Cao, G., Han, D., Yuan, H., Hu, Y., Shi, P., & Chen, Y. (2019). Deformation of the aquifer system under groundwater level fluctuations and its implication for land subsidence control in the Tianjin coastal region. *Environmental Monitoring and Assessment*, *191*(162), 1–14.

SUPPORTING INFORMATION

Additional supporting information may be found in the online version of the article at the publisher's website.

How to cite this article: Allocca, V., Coda, S., Calcaterra, D., & De Vita, P. (2022). Groundwater rebound and flooding in the Naples' periurban area (Italy). *Journal of Flood Risk Management*, *15*(2), e12775. https://doi.org/10.1111/jfr3.12775